EMBO reports

scientific report

MyRIP, a novel Rab effector, enables myosin VIIa recruitment to retinal melanosomes

Aziz El-Amraoui, Jean-Sébastien Schonn[1], Polonca Küssel-Andermann, Stéphane Blanchard, Claire Desnos[1], Jean-Pierre Henry[1], Uwe Wolfrum[2], François Darchen[1] & Christine Petit[+]

Unité de Génétique des Déficits Sensoriels, CNRS URA 1968, Institut Pasteur, 25 rue du Dr Roux, F-5724 Paris cedex 15, [1]CNRS UPR 1929, Institut de Biologie Physico-Chimique, 13 rue Pierre et Marie Curie, F-5005 Paris, France and [2]Institut für Zoologie, Johannes Gutenberg-Universität Mainz, D-55099 Mainz, Germany

Received January 1, 2002; revised and accepted March 1, 2002

Defects of the myosin VIIa motor protein cause deafness and retinal anomalies in humans and mice. We report on the identification of a novel myosin-VIIa-interacting protein that we have named MyRIP (myosin-VIIa- and Rab-interacting protein), since it also binds to Rab27A in a GTP-dependent manner. In the retinal pigment epithelium cells, MyRIP, myosin VIIa and Rab27A are associated with melanosomes. In transfected PC12 cells, overexpression of MyRIP was shown to interfere with the myosin VIIa tail localization. We propose that a molecular complex composed of Rab27A, MyRIP and myosin VIIa bridges retinal melanosomes to the actin cytoskeleton and thereby mediates the local trafficking of these organelles. The defect of this molecular complex is likely to account for the perinuclear mislocalization of the melanosomes observed in the retinal pigment epithelium cells of myosinVIIa-defective mice.

INTRODUCTION

Mutations in the *MYO7A* gene, encoding myosin VIIa, cause auditory and retinal defects in mice and humans (for a review, see Petit, 2001). The primary structure of myosin VIIa is highly conserved between vertebrates and invertebrates, with a motor head domain, a neck region composed of five IQ (isoleucine–glutamine) motifs, and a long tail region [1359 amino acids (aa) in man]. The tail begins with a dimerization domain, followed by two large repeats of ~460 aa, each containing a myosin tail homology 4 (MyTH4) and a 4.1, ezrin, radixin, moesin (FERM) domain, separated by a src homology type 3 (SH3) domain (Petit, 2001).

The myosin-VIIa-defective *shaker-1* mice are characterized by a progressive disorganization of the hair cell stereocilia, i.e. the stiff actin-filled microvilli forming the mechanoreceptive structure to sound stimulation (Self *et al.*, 1998). In the retina of *shaker-1* mice, melanosomes of the pigment epithelium cells are abnormally concentrated in the perinuclear region (Liu *et al.*, 1998), and opsin transport in the photoreceptor cells is delayed (Liu *et al.*, 1999; Wolfrum and Schmitt, 2000). Together, these observations point to the existence of several different roles for this unconventional myosin.

To gain insight into the cellular functions of myosin VIIa, we searched for proteins interacting with the myosin VIIa tail using the yeast two-hybrid system (Kussel-Andermann *et al.*, 2000a). We report here that myosin VIIa binds to a novel Rab effector protein that directly interacts with Rab27A, a Rab GTP-binding protein involved in the trafficking of skin melanosomes (for a review, see Marks and Seabra, 2001).

RESULTS

To identify proteins interacting with the tail of myosin VIIa, the C-terminal MyTH4 and FERM domains of the protein (last 464 aa) were used as the bait to screen a human retinal two-hybrid cDNA library (Kussel-Andermann *et al.*, 2000a). A prey composed of 418 aa encoded by clone A7 was considered to be a specific ligand of myosin VIIa, since no interaction could be observed with two control proteins, namely lamin C and merlin/schwannomin (which also possesses a FERM domain; see Supplementary figure 1 available at *Embo reports* Online). Using the A7 cDNA as a probe, a 5.2 kb transcript was detected in most human and mouse tissues tested, namely brain, kidney, heart, liver, muscle and pancreas (data not shown). A full-length cDNA, A7FL (DDBJ/EMBL/GenBank accession No. AF396687), was reconstituted from a human retinal cDNA library (see

[+]Corresponding author. Tel: +33 1 45 68 88 50; Fax: +33 1 45 67 69 78; E-mail: cpetit@pasteur.fr

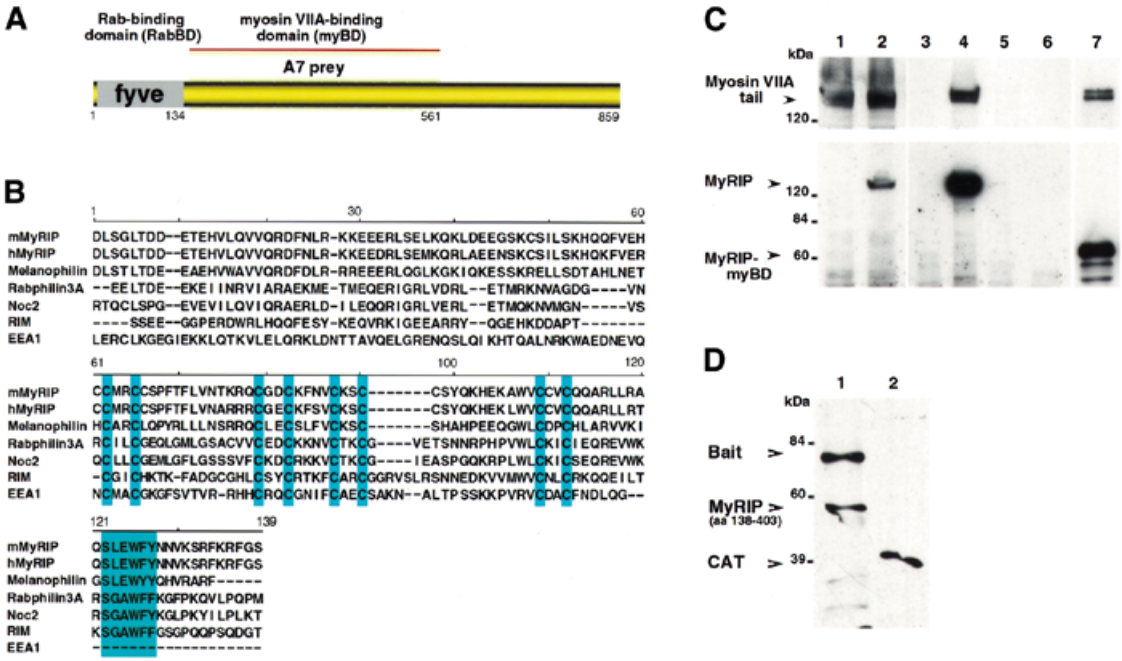

Fig. 1. MyRIP, a novel Rab effector that binds to myosin VIIa. (**A**) Structure of the MyRIP predicted protein. The N-terminal FYVE domain (Rab-binding domain) and the region corresponding to the A7 prey (i.e. binding to myosin VIIa) are indicated. (**B**) Clustal W sequence alignment of the FYVE domains of MyRIP and other Rab effectors. The eight conserved cysteine residues responsible for Zn^{2+} binding are indicated. The SGAWF(F/Y) motif that is involved in the binding of Rabphilin3A and Noc2 to Rab3A is shown. The MyRIP FYVE domain shows 50 and 30% aa identity with the Rab-binding domains of melanophilin and Rabphilin3A, respectively. (**C**) Immunoprecipitation experiment. Lane 1 contains soluble protein extract from HEK293 cells producing the myosin VIIa tail alone. Extracts from cotransfected HEK293 cells producing both the myosin VIIa tail and myc-MyRIP (lane 2) were used for immunoprecipitations (lanes 3 and 4). The two proteins are coprecipitated by the anti-hA7 MyRIP antibody (lane 4) but not by the corresponding preimmune serum (lane 3). Extracts from untransfected cells (lane 5) and from cells expressing the myosin VIIa tail alone (lane 6) were used as negative controls for the immunoprecipitation experiment with the anti-hA7 antibody. The myosin VIIa tail coprecipitated also with MyRIP–myBD, using the anti-hA7 antibody (lane 7). The mouse anti-myosin-VIIa (anti-SSI) and anti-myc (9E10) mouse monoclonal antibodies were used to detect the myosin VIIa tail (top), and the myc-MyRIP and myc-MyRIP–myBD (bottom), respectively. (**D**) *In vitro* binding assay. The bait (lane 1) and chloramphenicol acetyltransferase (CAT, lane 2)-bound resins were incubated with bacterial extracts containing a MyRIP fragment corresponding to aa 138–403. Only the bait binds to the MyRIP fragment. Horseradish-peroxidase-conjugated streptavidin was used to detect biotinylated proteins.

Methods). The deduced amino acid sequence predicts a 859 aa (96 kDa) protein (Figure 1A), hereafter named MyRIP (myosin-VIIa- and Rab-interacting protein) based on functional considerations (see below).

Sequence analysis of MyRIP revealed the existence of an N-terminal FYVE (Fab1p, YOTB, Vac1P, EEA1) domain (Figure 1A and B). The MyRIP FYVE domain, which is highly conserved between the human and murine proteins (95% aa identity), possesses the eight conserved cysteine residues (Figure 1B) that are known to coordinate the binding to two Zn^{2+} ions. Homology search analysis revealed an homology between the MyRIP FYVE domain and the Rab3-binding domain of Rabphilin3A, Rim and Noc2; and with the Slp homology domain (SHD) of two members of the synaptotagmin-like protein (Slp) family, Slp2 and Slp3 (30% aa identity), and Slac2a/melanophilin (50% aa identity; Figure 1B). The crystal structure of the Rabphilin3A FYVE domain complexed to Rab3A (Ostermeier and Brünger, 1999) has highlighted the involvement of a motif, SGAWF(F/Y), in the interaction with Rab3A (Figure 1B). Interestingly, a similar, although not identical, motif (SLEWFY) is present in MyRIP (Figure 1B). Accordingly, the MyRIP amino acid sequence can be subdivided into three regions, the N-terminal FYVE domain (aa 1–134), the myosin-VIIa-binding region (myBD, aa 143–560) and the C-terminal region (aa 561–859).

In order to confirm the interaction between myosin VIIa and MyRIP, HEK293 mammalian cells were cotransfected with constructs encoding the myosin VIIa tail and either the full-length MyRIP or the MyRIP–myBD truncated form. Coimmunoprecipitation of the myosin VIIa tail with either MyRIP or MyRIP–myBD (Figure 1C) was demonstrated on cell extracts incubated with an anti-MyRIP antibody (anti-hA7; see Methods). Furthermore, in a pull-down experiment, the myosin VIIa tail bound to the GST-tagged MyRIP–ΔCt (aa 1–561) fragment but not to GST alone (data not shown). In addition, an *in vitro* binding assay demonstrated a direct interaction between the 464 aa tail fragment of myosin VIIa corresponding to the original bait and a MyRIP fragment (Figure 1D). Taken together, these results demonstrate that MyRIP specifically binds to myosin VIIa.

The presence of a putative Rab-binding motif in the MyRIP sequence prompted us to search for Rab GTPases interacting with MyRIP. The interaction of different Rab proteins with immobilized GST-tagged MyRIP–RabBD, MyRIP–ΔCt or GST was measured by means of a filter binding assay. Significant bindings of Rab27A–GTP to MyRIP–RabBD and MyRIP–ΔCt were detected, as compared with immobilized GST (Figure 2A and B). Since Rab3 isoforms A, B, C and D, Rab4, Rab5, Rab6,

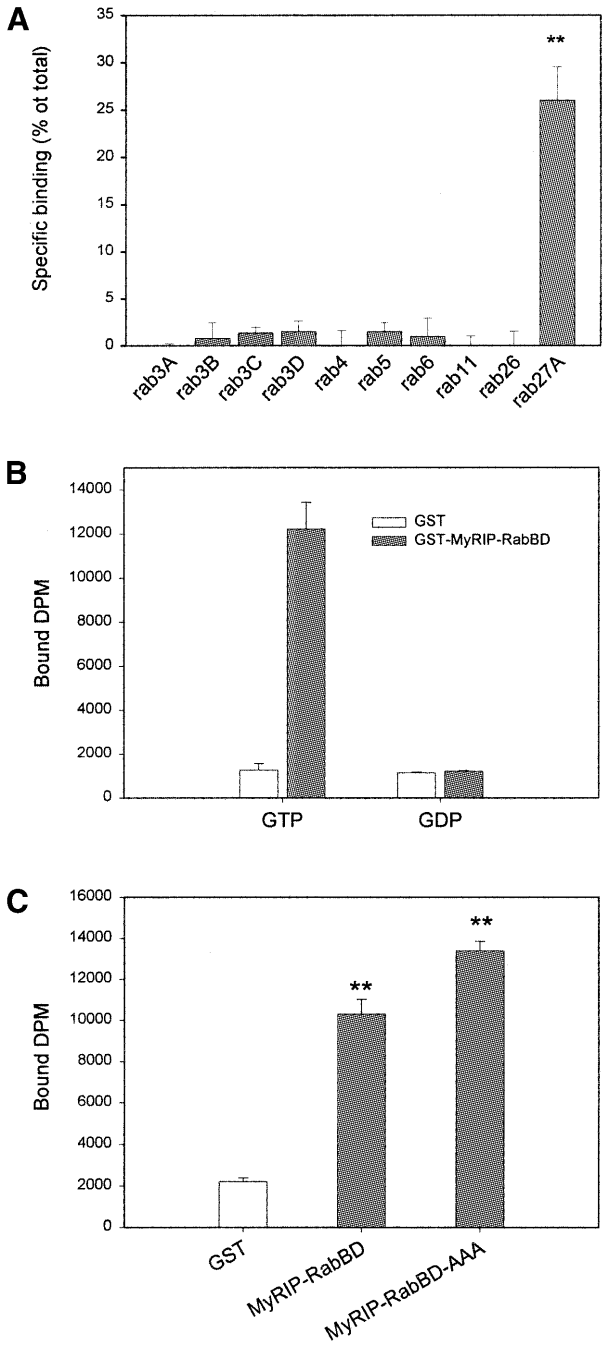

Fig. 2. MyRIP binds to Rab27A–GTP. (**A**) A filter binding assay was used to measure the binding of various Rab proteins to the GST-tagged MyRIP–RabBD. Non-specific binding to GST was subtracted. Only Rab27A binds to MyRIP–RabBD. (**B**) Recombinant Rab27A (80 nM) was loaded either with [^{3}H]GTP or [^{3}H]GDP and incubated with 150 pmol immobilized GST–MyRIP–RabBD (grey bars) or GST alone (white bars). Only GTP-bound Rab27A binds to MyRIP–RabBD. (**C**) Rab27A–GTP binds equally well to the mutated form MyRIP–RabBDAAA, carrying 3 aa substitutions in the SLEWFY motif. Data are shown as the percentage of the total radioactivity (mean ± SE, n = 3). ** indicates significant difference ($p < 0.01$) with the negative control GST.

Rab11 and Rab26 did not bind to MyRIP–RabBD (Figure 2A), the binding of Rab27A–GTP to MyRIP–RabBD was considered specific. This binding reached saturation, and a K_d of ~1 μM was derived (data not shown). Furthermore, Rab27A–GDP did not bind to MyRIP–RabBD, indicating that MyRIP specifically interacts with the GTP-bound form of Rab27A (Figure 2B). MyRIP–ΔCt exhibited no GTPase-activating protein (GAP) or guanine nucleotide exchange factor (GEF) activity (data not shown). The crystal structure of Rabphilin3A–Rab3A complex indicates that the SGAWFF motif (Figure 1B) constitutes one interface between Rabphilin3A and Rab3A molecules (Ostermeier and Brünger, 1999). Mutating this motif in Noc2 (SGAWFY to SGAAAA) impairs Noc2–Rab3A binding (Haynes *et al.*, 2001). In contrast, the mutation of the MyRIP SLEWFY motif to SLEAAA was not detrimental to the binding of MyRIP to Rab27A (Figure 2C).

Specific antibodies were generated against MyRIP (see Methods) and were used to analyse the distribution of the protein on mouse tissue sections. MyRIP was detected in a variety of tissues, including brain, skin, heart, adrenal medulla, pancreas, intestine, liver, kidney, muscle and testis (data not shown). The distribution of MyRIP was further analysed, using the anti-hA7 antibody, in the mouse inner ear and retina, i.e. the two target organs of the myosin VIIa defect in mice and humans. In the mouse inner ear, MyRIP was detected in the cochlear and vestibular hair cells, where it was colocalized with myosin VIIa in the synaptic region and along the hair cell bundle (data not shown). In the retina, MyRIP was present in the photoreceptor cells and pigment epithelium cells (Figure 3A), i.e. the two cell types where myosin VIIa has been detected (Hasson *et al.*, 1995; El-Amraoui *et al.*, 1996). In the photoreceptor cells, MyRIP was localized in the synaptic region. Ultrastructural analysis of MyRIP localization showed that the protein was present in both pre- and post-synaptic areas (data not shown). In the pigment epithelium cells, MyRIP and Rab27A were observed in the microvilli that surround the tips of the photoreceptor outer segments (Figure 3A and B; see Supplementary data). In addition, analysis of the subcellular distribution of MyRIP by immunoelectron microscopy showed the presence of gold particles on melanosomes (Figure 3C and D). Myosin VIIa (Figure 3E; Liu *et al.*, 1998) and Rab27A (Figure 3F) were also associated with retinal melanosomes.

Since MyRIP was present also in the synaptic areas of retinal photoreceptor cells (Figure 4A) and inner ear hair cells, we used the PC12 neuroendocrine cell line to determine whether MyRIP is able to recruit the myosin VIIa tail upon cotransfection. In differentiated PC12 cells producing GFP–myosin-VIIa tail, a punctate labelling of the cell body was observed, whereas the neurites were almost unstained (Figure 4A). In contrast, in PC12 cells expressing both the GFP–myosin-VIIa tail and myc-MyRIP, the myosin VIIa tail was enriched significantly at the tip of the neurites (Figure 4B). This enrichment appeared specific, since it was not observed upon cotransfection with a construct encoding either a MyRIP truncated form, lacking the Rab-binding protein, or the myc-tagged fruitfly luciferase (data not shown). We then examined the involvement of each of the three MyRIP regions in the protein targeting (Figure 4C). We found that, in PC12 cells expressing a MyRIP–RabBD construct, MyRIP–RabBD labelling was observed essentially at the tip of the neurites (Figure 4E, arrows), reminiscent of that observed in cells producing full-length MyRIP. In contrast, no such enrichment

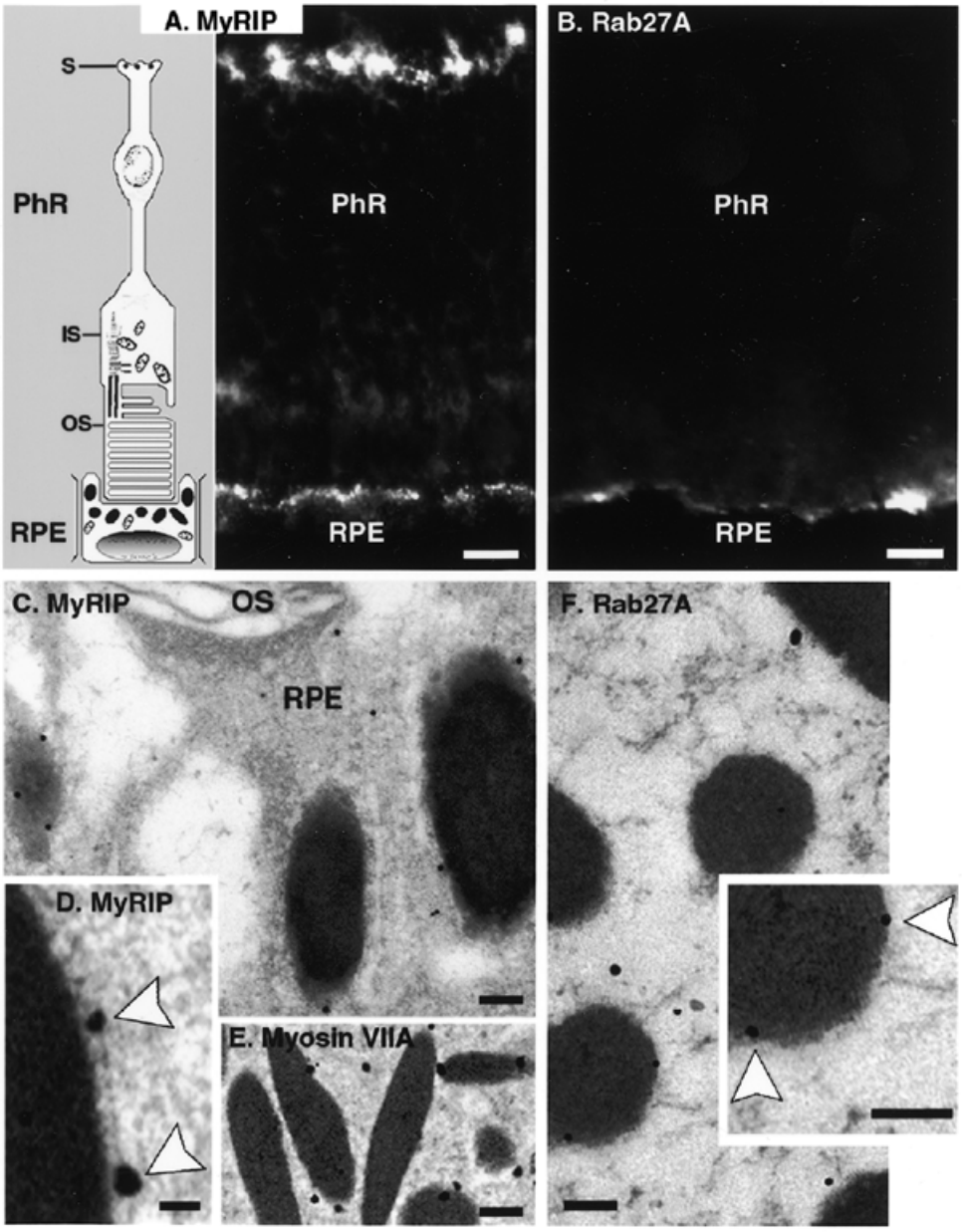

Fig. 3. Localization of MyRIP and Rab27A in the mouse retina. (**A**) MyRIP is detected at the synaptic region (S) of photoreceptor cells (PhR) and on the microvilli of retinal pigment epithelium (RPE) cells. (**B**) Rab27A is present on the microvilli of RPE cells. In RPE cells, MyRIP (**C** and **D**), myosin VIIa (**E**) and Rab27A (**F**) silver-enhanced immunogold labellings are associated with the membrane of melanosomes. IS, inner segment; OS, outer segment. Scale bars: (A and B), 12 μm; (C), 175 nm; (D), 100 nm; (E), 235 nm; (F and inset), 140 nm.

was observed at the tips of the neurites in cells producing either MyRIP–myBD, MyRIP–ΔRabBD or MyRIP–Ct (Figure 4D and F). Together, these results show that the targeting of MyRIP to the synaptic regions at the tip of the neurites is mediated by its Rab-binding domain. They also show that MyRIP is able to promote the recruitment of myosin VIIa at these emplacements.

DISCUSSION

We have identified a novel Rab effector protein, MyRIP, that binds to myosin VIIa. Several lines of evidence argue in favour of MyRIP providing a link between the actin cytoskeleton and organelles: (i) MyRIP directly interacts with the actin-based motor protein myosin VIIa and with Rab27A; (ii) MyRIP, Rab27A and myosin VIIa are detected on retinal melanosomes; and (iii) MyRIP is able to interfere with myosin VIIa tail localization and, in particular, to promote its recruitment, via the Rab-binding domain, to the tip of the neurites in differentiated PC12 cells.

Previous studies have implicated Rab27A in the transport of the skin melanosomes (Marks and Seabra, 2001). Mutations of *Rab27a* were found in *ashen* mutant mice, which exhibit clumping of melanosomes in the perinuclear region of skin

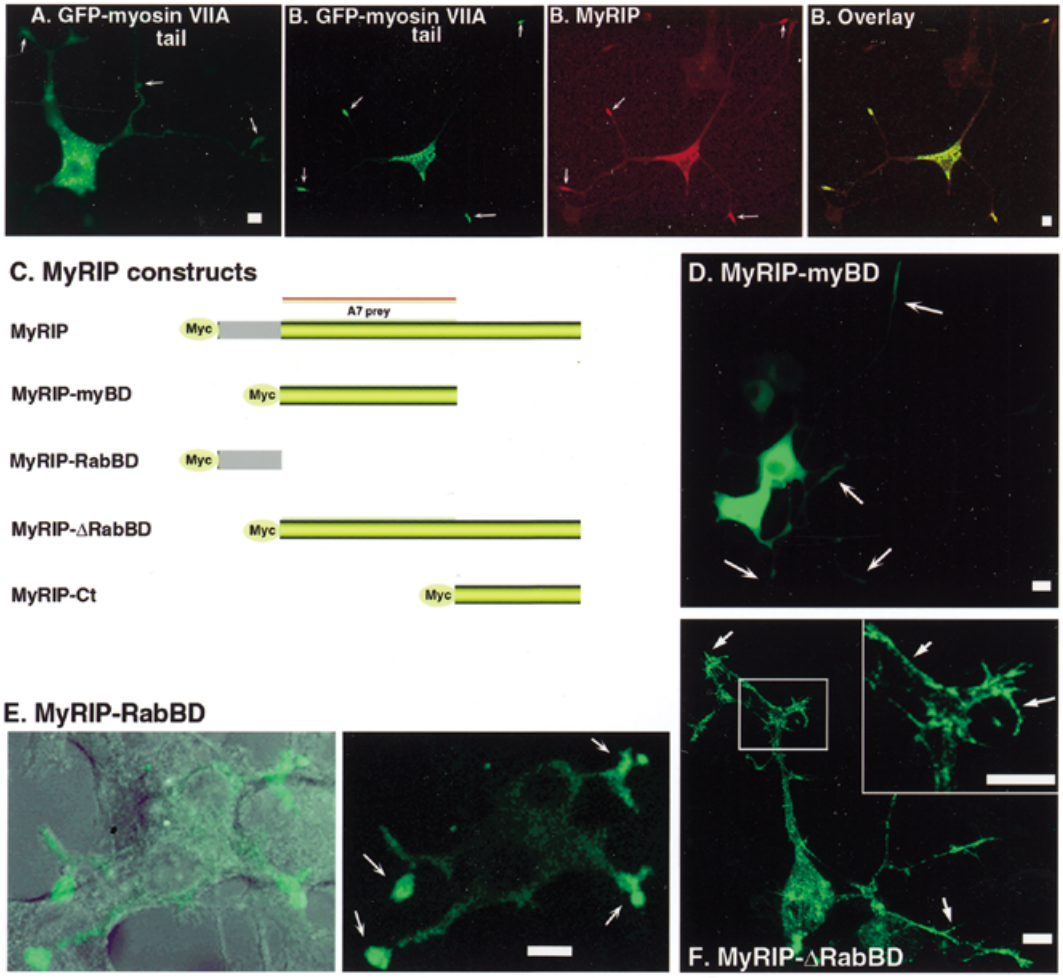

Fig. 4. In PC12 cells producing the GFP–myosin-VIIa tail alone (**A**), the labelling is observed essentially in the cell body, whereas the neurites are unstained (arrows). In contrast, in PC12 cells coproducing MyRIP and the GFP–myosin-VIIa tail (**B**), the two proteins are entirely colocalized not only in the cell body, but also at the tip of the neurites (arrows). Different MyRIP truncated forms (**C**) are produced in PC12 cells. In PC12 cells producing MyRIP–myBD (**D**), a cytosolic diffuse labelling is observed in the cell body; no labelling is detected at the neurite tips (arrows). In contrast, in cells producing MyRIP–RabBD (**E**), an enrichment of the immunolabelling is observed at the tip of the neurites (arrows). No such enrichment is observed in PC12 cells producing MyRIP–ΔRabBD (**F**); immunolabelling is associated with several spines extending from the neurites (arrows). The myc-tagged MyRIP fusion proteins are detected using the anti-myc (9E10) antibody. Scale bar = 10 μm.

melanocytes (Wilson *et al.*, 2000), and in patients affected by Griscelli syndrome, which associates with partial albinism and immunodeficiency (Menasche *et al.*, 2000). Myosin Va has also been shown to be involved in melanosome trafficking, since *Myo5a* mutations have been identified both in *dilute* mice, which exhibit defects in the trafficking of skin melanosomes (Mercer *et al.*, 1991), and in patients affected by Griscelli syndrome (Pastural *et al.*, 2000). Moreover, several studies on skin melanocytes have led to the conclusion that Rab27A recruits myosin Va onto melanosomes and thereby enables the capture and local actin-based movement of these organelles towards the cell periphery (Bahadoran *et al.*, 2001; Hume *et al.*, 2001; Wu *et al.*, 2001). These studies thus demonstrate that myosin Va and Rab27A are part of a melanosome trafficking machinery. However, it is not yet clear whether these molecules bind directly to each other. Our results show that MyRIP provides a physical link between Rab27A, on the retinal melanosome membrane, and the actin-based motor molecule myosin VIIa. We propose that myosin VIIa, MyRIP and Rab27A act together to coordinate the short range peripheral movement of melanosomes along the actin-rich microvilli of retinal pigment epithelium cells (Figure 5). As a corollary, the loss of a functional myosin-VIIa–MyRIP–Rab27A complex is likely to account for the perinuclear accumulation of the melanosomes observed in the retinal cells of myosin-VIIa-defective *shaker-1* mice (Liu *et al.*, 1998). However, *shaker-1* mice do not exhibit visual impairment, which indicates that the proper localization of the retinal melanosomes is not required for retinal viability.

During the completion of this study, Matesic *et al.* (2001) reported that *leaden*, another coat pigmentation mouse mutant, results from a defect in Slac2a/melanophilin, and Kuroda *et al.* (2002) found that Slac2a/b and Slp1-4 interact with Rab27A. MYRIP and melanophilin show no homology, and melanophilin lacks the region that, in MyRIP, binds to myosin VIIa. However,

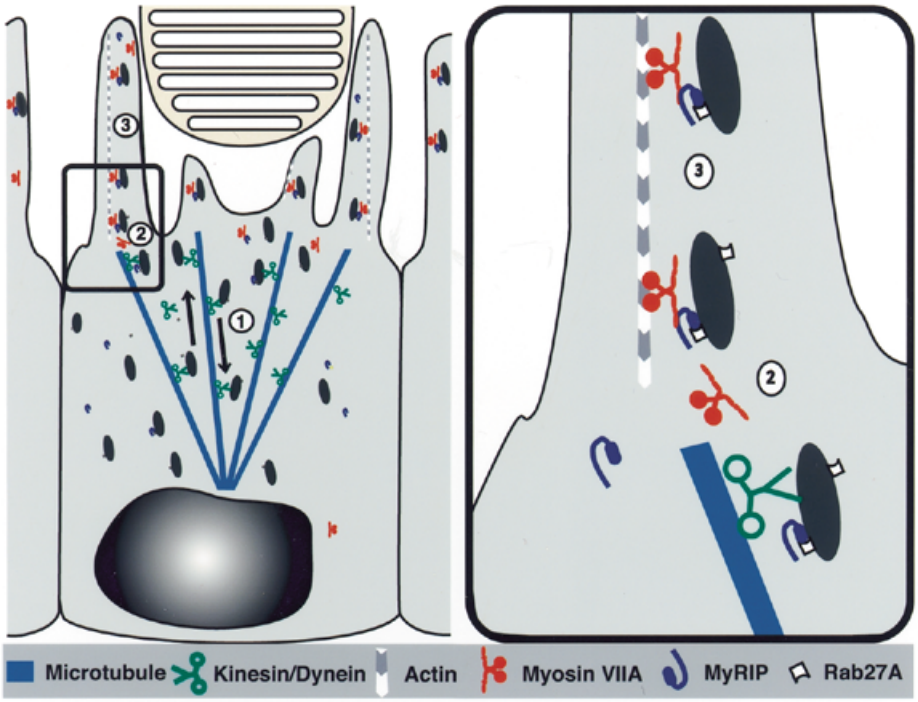

Fig. 5. Model of the trafficking of melanosomes in the retinal pigment epithelium cells. (1) Melanosomes display fast, bidirectional, microtubule-dependent long-range movements in the cell body. (2) Rab27A targeted to the melanosome membrane interacts with its effector, MyRIP, which in turn binds to the actin-based motor protein myosin VIIa. (3) Myosin VIIa then enables the local movement of the melanosomes along the actin filaments of the microvilli.

the two proteins shared similar FYVE domains, both of which contain two Zn^{2+}-binding sites followed by a SLEW(F/Y)Y motif (see Figure 1B). Slac2b and Slp1-4 also possess a similar motif in their SHD2 domain, e.g. SGQWFY in Slp2 protein (Kuroda *et al.*, 2002). We show here that mutating the SLEWFY motif of MyRIP does not impair its binding to Rab27A. The MyRIP–Rab27A interaction thus may involve the N-terminal α-helical segment, upstream of the Zn^{2+}-binding sites, a region that has been shown to mediate Rim–Rab3A binding (Sun *et al.*, 2001; Wang *et al.*, 2001). Interestingly, the melanophilin defect in *leaden* mice is due to the deletion of 7 aa (REEERLQ) between aa 31 and 37, i.e. within the corresponding α-helical segment of the protein (Matesic *et al.*, 2001). Similar amino acids are observed in MyRIP (KEEERLS, aa 31–37), Rim (TEEERNI, aa 29–35), Slac2b and Slps, thus suggesting that the Rab-binding sites of all these proteins are located within their N-terminal α-helical domain (or SHD1 domain, according to Kuroda *et al.*, 2002). By analogy with the interactions described here, we consider that the *leaden* phenotype is likely due to a disruption of melanophilin binding to Rab27A. In any case, the finding that *leaden* results from a defective MyRIP-related protein supports our proposal that MyRIP is involved in melanosome trafficking. Therefore, peripheral melanosome trafficking in retinal pigment epithelium cells and in skin melanocytes would depend on the same Rab protein, Rab27A, but would involve two different motor proteins, myosin VIIa and myosin Va, respectively.

The presence of MyRIP in the synaptic areas of inner ear hair cells and retinal photoreceptor cells suggests that this protein is involved in the trafficking of other organelles, including synaptic vesicles. In PC12 cells, MyRIP is able to target the myosin VIIa tail to the tips of the neurites, where secretory vesicles are concentrated. Preliminary data suggest that MyRIP is associated with secretory vesicles in these cells. Interestingly, when the myosin VIIa tail is coexpressed with MyRIP lacking the Rab-binding domain, MyRIP–ΔRabBD, the two proteins perfectly colocalized in PC12 cells, but no enrichment was observed at the tips of the neurites. Therefore, MyRIP–RabBD likely mediates the targeting of MyRIP–myosin-VIIa complex to the tip of the neurites. Although we still do not know whether Rab27A is present at the tip of these neurites, in the retinal pigment epithelium cells, the localization of the three proteins at the apical cell microvilli strongly suggests that Rab27A recruits the MyRIP–myosin-VIIa complex via an interaction with MyRIP–RabBD. Finally, MyRIP is expressed in wide range of tissues, among which some lack Rab27A and/or myosin VIIa (i.e. muscle, heart and brain). The here-described dynamic module and its likely variant, made up myosin-V–melanophilin–Rab27A, led us to put forward the idea that unconventional myosin/myosin- and Rab-binding protein/Rab form a sort of basic recognition unit. Heterogeneity of this unit may underlie its contribution to different steps of vesicle trafficking. Since we propose Rab27A as a component of two of them, the possibility that also melanophilin and MyRIP belong to different modules is worth considering.

METHODS

MyRIP and other expression constructs. Yeast two-hybrid screening of a human retinal library was performed as described previously (Kussel-Andermann *et al.*, 2000a). The cDNA of clone A7 was used to isolate the MyRIP full-length cDNA from

a retinal cDNA library in λgt11 (Clontech). The mouse MyRIP cDNA (DDBJ/EMBL/GenBank accession No. AF396688) was obtained by 5′ RACE–PCR using an inner ear Marathon cDNA. Oligonucleotides designed from the rat EST226177 clone were used for amplification.

The MyRIP full-length coding sequence (aa 1–859) was PCR-amplified from human retina Marathon cDNA and subcloned in the pCMV–tag3B vector (Clontech). The following myc-tagged MyRIP truncated constructs were generated: pCMV3B–MyRIP–RabBD (aa 1–134); pCMV3B–MyRIP–ΔRabBD (aa 138–859); pCMV3B–MyRIP–myBD (aa 138–568); and pCMV3B–MyRIP–Ct (aa 561–859). The mutant form of the MyRIP–RabBD was generated by PCR amplification. The GFP–myosin-VIIa tail construct has been described previously (Kussel-Andermann *et al.*, 2000b).

Anti-MyRIP antibodies. Three different anti-MyRIP polyclonal antibodies were generated in the rabbit: anti-hA7 was raised against a His_6-tagged A7 fusion protein derived from the human MyRIP sequence (aa 186–383); and anti-mA7 was raised against a His_6-tagged A7 fusion protein derived from the murine MyRIP sequence (aa 110–305); anti-hA7P was raised against a peptide, hA7P: EAPSRQPRDQGQHPRC, derived from the human MyRIP sequence (aa 310–324). The specificity of the three immuno-purified antibodies (anti-hA7, anti-hA7P and anti-mA7) was checked by immunoblot and immunofluorescence analyses.

Binding experiments. For immunoprecipitation experiments, the myosin VIIa tail (aa 847–2215) was cloned in the pcDNA3 vector (Invitrogen). For the production of GST–MyRIP fusion proteins, the following constructs were subcloned in the pGEX-4T1 vector (Pharmacia): pGEX-RabBD (aa 1–134) and pGEX-MyRIP–ΔCt (aa 1–568). For the production of biotinylated MyRIP, a fragment of MyRIP–myBD corresponding to aa 138–403 was subcloned into the pXa3 vector (Promega). The *in vitro* binding and pull-down experiments were performed as described previously (Kussel-Andermann *et al.*, 2000a).

Immunohistofluorescence and electron microscopy analysis. PC12 cells and mouse tissues were fixed with 4% paraform-aldehyde and processed for indirect immunofluorescence microscopy as described previously (El-Amraoui *et al.*, 1996). Immunoelectron microscopy was performed on LR White embedded ultra-thin sections of mouse retina as described previously (Wolfrum and Schmitt, 2000). The monoclonal mouse anti-Rab27A was obtained from Transduction Laboratories.

Filter binding assay. Purified Rab proteins (40–120 nM) were loaded with [^{3}H]GTP (7.7 Ci/mmol, Amersham) and incubated with 150 pmoles of GST or GST-fusion proteins immobilized on glutathione–Sepharose in 20 mM Tris–HCl pH 8.0, 150 mM NaCl, 1 mM $MgCl_2$, 1 mM dithiotreitol and 50 µM Zn acetate. The mixture (30–50 µl) was kept on ice for 15 min. The reaction was terminated by the addition of 3 ml washing buffer (20 mM Tris–HCl pH 8.0, 100 mM NaCl, 1 mM $MgCl_2$) and filtration through glass-fibre filters (Whatman GF/C) preincubated in washing buffer supplemented with 0.5% bovine serum albumin. After three washes, the filters were processed for scintillation counting.

Supplementary data. Supplementary data are avaliable at *EMBO reports* Online.

ACKNOWLEDGEMENTS

We thank J.-P. Hardelin and S. Safieddine for critical reading of the manuscript, J. Levilliers for her continuous help and R. Schäfer for technical assistance. We thank G. Baldini, M. Cormont, J. Salaméro, M. Zerial, B. Goud, H. Shimomura and G. de Saint Basile for their kind gift of vectors encoding Rab3D, Rab4, Rab5, Rab6, Rab11, Rab26 and Rab27A, respectively. This work was supported by grants from EC (QLG2-CT-1999-00988), R. and G. Strittmatter, Retina-France, A. and M. Suchert, Forschung contra Blindheit-Initiative Usher Syndrome, Deutsche Forschungsgemeinschaft (Wo548/3 and /4) and FAUN-Stiftung (to U.W.).

REFERENCES

Bahadoran, P. *et al*. (2001) Rab27a: a key to melanosome transport in human melanocytes. *J. Cell Biol.*, **152**, 843–849.

El-Amraoui, A., Sahly, I., Picaud, S., Sahel, J., Abitbol, M. and Petit, C. (1996) Human Usher IB/mouse *shaker-1*: the retinal phenotype discrepancy explained by the presence/absence of myosin VIIa in the photoreceptor cells. *Hum. Mol. Genet.*, **5**, 1171–1178.

Hasson, T., Heintzelman, M.B., Santos-Sacchi, J., Corey, D.P. and Mooseker, M.S. (1995) Expression in cochlea and retina of myosin VIIa, the gene product defective in Usher syndrome type 1B. *Proc. Natl Acad. Sci. USA*, **92**, 9815–9819.

Haynes, L.P., Evans, G.J., Morgan, A. and Burgoyne, R.D. (2001) A direct inhibitory role for the Rab3-specific effector, Noc2, in Ca^{2+}-regulated exocytosis in neuroendocrine cells. *J. Biol. Chem.*, **276**, 9726–9732.

Hume, A.N., Collinson, L.M., Rapak, A., Gomes, A.Q., Hopkins, C.R. and Seabra, M.C. (2001) Rab27a regulates the peripheral distribution of melanosomes in melanocytes. *J. Cell Biol.*, **152**, 795–808.

Kuroda, T.S, Fukuda, M., Ariga, H., and Mikoshiba, K. (2002) The Slp homology domain of synaptotagmin-like proteins 1–4 and Slac2 functions as a novel Rab27A binding domain. *J. Biol. Chem.*, **277**, 9212–9218

Kussel-Andermann, P., El-Amraoui, A., Safieddine, S., Hardelin, J.P., Nouaille, S., Camonis, J. and Petit, C. (2000a) Unconventional myosin VIIa is a novel A-kinase-anchoring protein. *J. Biol. Chem.*, **275**, 29654–29659.

Kussel-Andermann, P., El-Amraoui, A., Safieddine, S., Nouaille, S., Perfettini, I., Lecuit, M., Cossart, P., Wolfrum, U. and Petit, C. (2000b) Vezatin, a novel transmembrane protein, bridges myosin VIIa to the cadherin–catenins complex. *EMBO J.*, **19**, 6020–6029.

Liu, X., Ondek, B. and Williams, D.S. (1998) Mutant myosin VIIa causes defective melanosome distribution in the RPE of *shaker-1* mice. *Nature Genet.*, **19**, 117–118.

Liu, X., Udovichenko, I.P., Brown, S.D., Steel, K.P. and Williams, D.S. (1999) Myosin VIIa participates in opsin transport through the photoreceptor cilium. *J. Neurosci.*, **19**, 6267–6274.

Marks, M.S. and Seabra, M.C. (2001) The melanosome: membrane dynamics in black and white. *Nature Rev. Mol. Cell. Biol.*, **2**, 738–748.

Matesic, L.E., Yip, R., Reuss, A.E., Swing, D.A., O'Sullivan, T.N., Fletcher, C.F., Copeland, N.G. and Jenkins, N.A. (2001) Mutations in Mlph, encoding a member of the Rab effector family, cause the melanosome transport defects observed in *leaden* mice. *Proc. Natl Acad. Sci. USA*, **98**, 10238–10243.

Menasche, G. *et al*. (2000) Mutations in RAB27A cause Griscelli syndrome associated with haemophagocytic syndrome. *Nature Genet.*, **25**, 173–176.

Mercer, J.A., Seperack, P.K., Strobel, M.C., Copeland, N.G. and Jenkins, N.A. (1991) Novel myosin heavy chain encoded by murine dilute coat colour locus. *Nature*, **349**, 709–713.

Ostermeier, C. and Brünger, A.T. (1999) Structural basis of Rab effector specificity: crystal structure of the small G protein Rab3A complexed with the effector domain of rabphilin-3A. *Cell*, **96**, 363–374.

Pastural, E. *et al*. (2000) Two genes are responsible for Griscelli syndrome at the same 15q21 locus. *Genomics*, **63**, 299–306.

Petit, C. (2001) Usher syndrome: from genetics to pathogenesis. *Annu. Rev. Genomics Hum. Genet.*, **2**, 271–297.

Self, T., Mahony, M., Fleming, J., Walsh, J., Brown, S.D. and Steel, K.P. (1998) *Shaker-1* mutations reveal roles for myosin VIIa in both development and function of cochlear hair cells. *Development*, **125**, 557–566.

Sun, L., Bittner, M.A., Holz, R.W. and Araki, K. (2001) Rab3a binding and secretion-enhancing domains in Rim1 are separate and unique. Studies in adrenal chromaffin cells. *J. Biol. Chem.*, **276**, 12911–12917.

Wang, X., Hu, B., Zimmermann, B. and Kilimann, M.W. (2001) Rim1 and Rabphilin-3 bind Rab3–GTP by composite determinants partially related through N-terminal α-helix motifs. *J. Biol. Chem.*, **276**, 32480–32488.

Wilson, S.M. *et al*. (2000) A mutation in Rab27a causes the vesicle transport defects observed in *ashen* mice. *Proc. Natl Acad. Sci. USA*, **97**, 7933–7938.

Wolfrum, U. and Schmitt, A. (2000) Rhodopsin transport in the membrane of the connecting cilium of mammalian photoreceptor cells. *Cell Motil. Cytoskeleton*, **46**, 95–107.

Wu, X., Rao, K., Bowers, M.B., Copeland, N.G., Jenkins, N.A. and Hammer, J.A. (2001) Rab27a enables myosin Va-dependent melanosome capture by recruiting the myosin to the organelle. *J. Cell Sci.*, **114**, 1091–1100.

DOI: 10.1093/embo-reports/kvf090